We are IntechOpen,
the world's leading publisher of
Open Access books
Built by scientists, for scientists

4,800
Open access books available

122,000
International authors and editors

135M
Downloads

Our authors are among the

154
Countries delivered to

TOP 1%
most cited scientists

12.2%
Contributors from top 500 universities

CLARIVATE ANALYTICS
BOOK CITATION INDEX
INDEXED

WEB OF SCIENCE™

Selection of our books indexed in the Book Citation Index
in Web of Science™ Core Collection (BKCI)

Interested in publishing with us?
Contact book.department@intechopen.com

CFD Analysis of Flow Characteristics in a Jet Laryngoscope and the Different Application Forms of Superimposed Jet Ventilation

Alexander Aloy, Simon Hell, Andreas Nowak and Matthaeus Grasl

Abstract

The superimposed high-frequency jet ventilation is a jet ventilation technique that allows the surgeon to operate in a system open to the outside endoscopic surgery in the area of the vocal cord level. Although the clinical application is uncomplicated, the possible mechanisms of the gas flow in the jet laryngoscope are largely unknown. In the performed calculations for this work, the CFD software package Fluent is used with the preprocessor GAMBIT. After creating the geometry and networking of the jet laryngoscope in the preprocessor GAMBIT, the boundary conditions and input parameters in the solver are defined. This is followed by iterative calculation using Fluent and the tabulation of results. Ventilation is provided by an electronic respirator specially developed for the endoscope. There is a bidirectional gas flow in the jet laryngoscope. The free jet characteristics of the jet beam can be confirmed. Entrainment depends on pressure and on the gas velocity. The arrangement of the nozzles enables jet ventilation in stenosis. CFD analysis enables the representation of a continuous progress of the pressure as well as the representation of the continuous profile of the velocity in the investigated endoscope. Additionally the practical application for intensive care ventilation is shown.

Keywords: jet ventilation, superimposed high-frequency jet ventilation (SHFJV), computational fluid dynamics (CFD), laryngeal stenosis, jet respirator, combined high-frequency jet ventilation, flow behavior

1. Introduction

Jet ventilation in medicine means the administration of small to the smallest gas volumes (1–2 ml/kilogram per body weight) with a high frequency from a nozzle or special adaptors to ventilate a patient. This ventilation is used in surgical surgery as well as in intensive care medicine. In contrast to the dynamics of a sustained flight jet beam, the jet stream in medical application is only supposed to expand the

lung during the inspiratory phase. Thereafter, the expiration should be passively carried out by sifting the air supply. But in the expiratory phase, the air should not be completely exhaled. A positive end-expiratory pressure (PEEP) should prevent a collapse of alveoli. In case of surgery on the larynx as well as in the trachea, both the surgeon and the anesthetist interfere in the same working area. An often used endotracheal tube ensures the mechanical ventilation and, however, represents a massive disability for the surgeon. One possibility is the use of thin endotracheal tubes to provide the surgeon more space for his operational activity. Alternatively, however, techniques were developed in which the gas flows without endotracheal tube through the surgical area directly into the trachea. One possibility is the use of an endoscope in which nozzles for jet ventilation are integrated. The gas emerging from the nozzles flows through the endoscope and through the vocal cord plane into the trachea.

Computational fluid dynamics (CFD), a viable method for analyzing flow behavior, is well established for the investigation [1] of fluid mechanics. In recent years this method has been applied in the medical field to better understanding the behavior of gas currents in the human lung [2, 3]. Furthermore, technical issues related to mechanical ventilation can be solved by CFD. High-frequency ventilation (high-frequency jet ventilation, jet ventilation) is a ventilation technique that is characterized by the application of a small tidal volume through a variable nozzle, usually at high frequency [4]. Jet ventilation enables the transport and administration of small volumes of compressed gas at high pressures through a thin catheter or small metal tubes whose ends have the characteristics of a nozzle. However, the use of tubes or catheters involves the risk of dislocation or kinking, with the subsequent obstruction of the gas flow [5–7].

Superimposed high-frequency jet ventilation (SHFJV) is a simultaneous, combined application of low- and high-frequency jet ventilations [8]. Jet ventilation is characterized by the appearance of some physical effects whose characteristics make them feasible for mechanical ventilation in endoscopic surgery. One of these effects is the free jet character of the gas flow. The respiratory gas is to be transported in an outward open system from the jets through the vocal cord level in the lung. After the exit of the gas from the nozzle, it moves at the SHFJV over a short distance as a free jet in the direction of the vocal cord level. When the gas leaves the nozzle, the energy of the gas is sufficient to produce a forward pressure thrust. The gas then flows with a reduced controllable pressure needed for mechanical ventilation through the endoscope and glottis into the lungs. Another characteristic of this free jet is an entrainment [9] of the surrounding air. Thus, the enriched oxygen gas coming out of the jet is reduced in its concentration. These physical effects are applicable to jet ventilation and in particular for the superimposed high-frequency jet ventilation. Although this technique was initially developed for operations on the vocal cords in adults, the spectrum of this technology has expanded. Thus, this technique is particularly suitable for children, because of the limited space and the difficult working conditions for the surgeon. Furthermore, the operating range has been extended to the subglottic space and tracheal space. The anatomical relationships are not changed. Another crucial aspect is the use of jet ventilation in high-grade stenosis [10, 11]. The localization of these pathological changes which lead to a reduction in cross section for the gas flow can be localized above, directly in the vocal cord or even below. From a medical-technical point of view, it is necessary to administer the gas jet with a higher pressure in order to maintain a sufficient tidal volume behind the stenosis in the lung. At the same time, however, it must be ensured that the applied gas volume behind the stenosis does not lead to hyperinflation of the lungs. Hyperinflation of the lungs can cause barotrauma due to a blockage of the gas outflow. The question that arises is can

the pressure behind the stenosis be higher than the pressure before the stenosis, with this ventilation technique? Current clinical results show that in no case a barotrauma occurred even in cases of severe stenosis [12]. However, publicized data on the validation of the general gas behavior and flow patterns within the jet laryngoscopes is still absent in the literature. The aim of this study was to analyze fluid dynamic processes within the jet laryngoscope by a flow simulation. The behavior of the combined low- and high-frequency jets should be investigated in the endoscope. The entrainment of the gas caused by the two jets with the characteristics of free flow is to be analyzed in its behavior. Subsequently, the behavior of the distribution of the flow and the pressure in a stenosis is to be examined. The potential risk for barotrauma using supraglottic jet ventilation in the presence of a stenosis is to be investigated.

## 1.1 Material and methods

1.1.1 Jet laryngoscope

The jet laryngoscope (comp. Carl Reiner, Vienna, Austria) contains two metal jets welded to the side of the endoscope. The jets are directed downward and end at the inside wall of the laryngoscope with an opening into the lumen. The alignment of each jet stream is based on an imaginary center of the distal end of the laryngoscope, implying that this stream is continued along a median line into the trachea. The openings of the jet nozzles are positioned in the upper third of the endoscope and not at the top of the endoscope. An additional line is affixed to the right side of the laryngoscope. This line ends at the tip of the laryngoscope and solely served to pressure monitoring. Two jet streams with different frequencies were applied simultaneously. The continuous high-frequency jet stream is applied during expiration period and superimposed during the inspiratory phase of the low-frequency jet ventilation. The low-frequency jet stream resulted in phased airway pressure changes analogous to conventional ventilation with 12–20 bpm and provided the upper (higher) pressure level. The high-frequency jet stream has a frequency of 100–1500 cycles/min and is creating the lower pressure level corresponding to a positive end-expiratory pressure (PEEP). The released gas has a pressure of 1–1.5 bar, which declines hundredfold upon reaching the vocal cords resulting in a pressure of 10–15 mbar at the distal endoscope opening. The two jet streams are administered by an electronic respirator (**Figure 1**).

1.1.2 Geometry of the model

For creation of a geometry model, GAMBIT software was used. To reduce computing time, minor simplifications to the model had to be made. The entry and exit diameters of the laryngoscope were approximated to an elliptical form (entry, a = 13 mm and b = 8 mm; exit, a = 7 mm and b = 4 mm; a and b are the semiaxes of the ellipses). The nozzles were depicted as section planes in Fluent to ensure accurate depiction of peripheral airflow conditions. The total length of the laryngoscope was 165 mm, and the angle of oxygen entry was 28°, while the distance between nozzle and gas release diameter was 48 mm for low-frequency and 68 mm for high-frequency ventilation. The inner nozzle diameter was 1.7 mm.

1.1.3 The network model

Connection simulation (**Figure 2**) was also done by GAMBIT software in the following manner: Firstly, the segments immediately before and after the
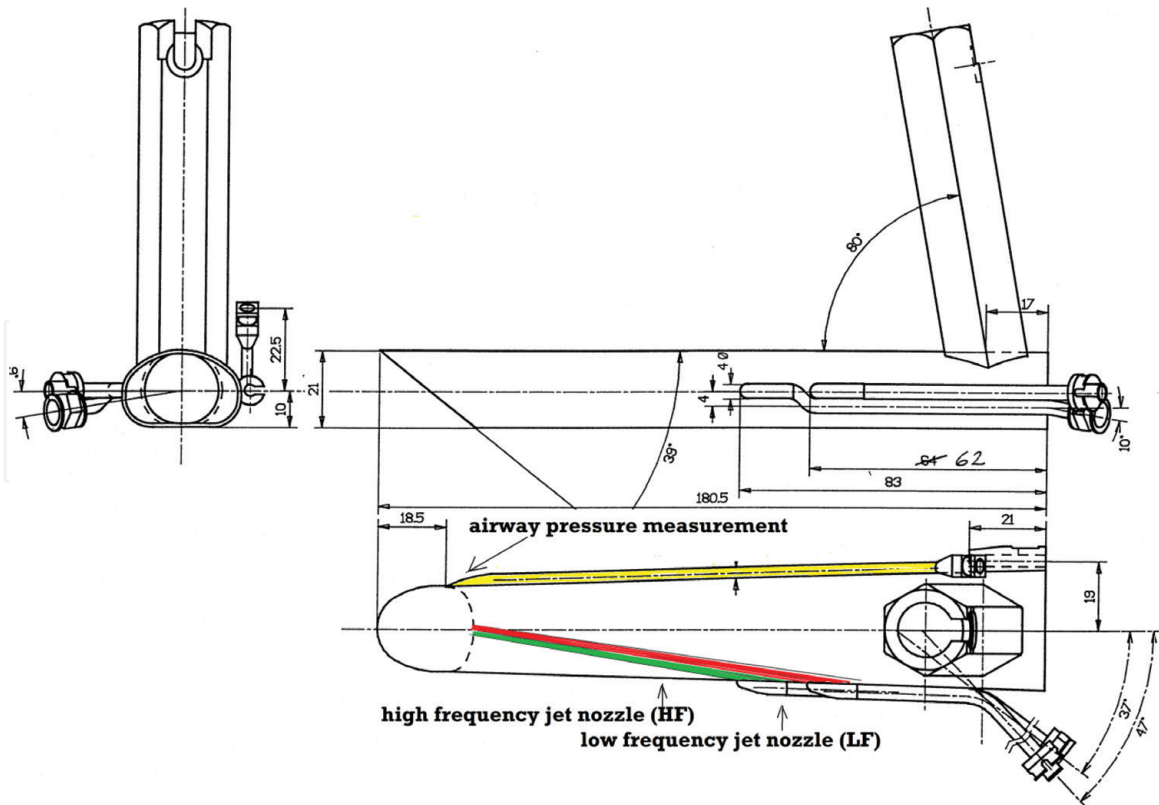
Figure 1.
Schematic description of the jet laryngoscope: Localizations of the jets and airway pressure measurement (yellow).

laryngoscope entrance and exit diameter were configured according to the Cooper regimen. The front surfaces were connected to the elements of Hex/Hedge type. This implies that hexahedral (six-sided) elements were primarily used, unless wedge elements were required. For the middle segment, the Cooper regimen could not be used, because of the presence of the nozzles. The elements were connected according to the Pave system, which is not compatible with the Cooper regimen. This area around the nozzles was analyzed with higher resolution, because of the essential character of this area for the results of our study. An edge plane was applied to the wall of the laryngoscope.
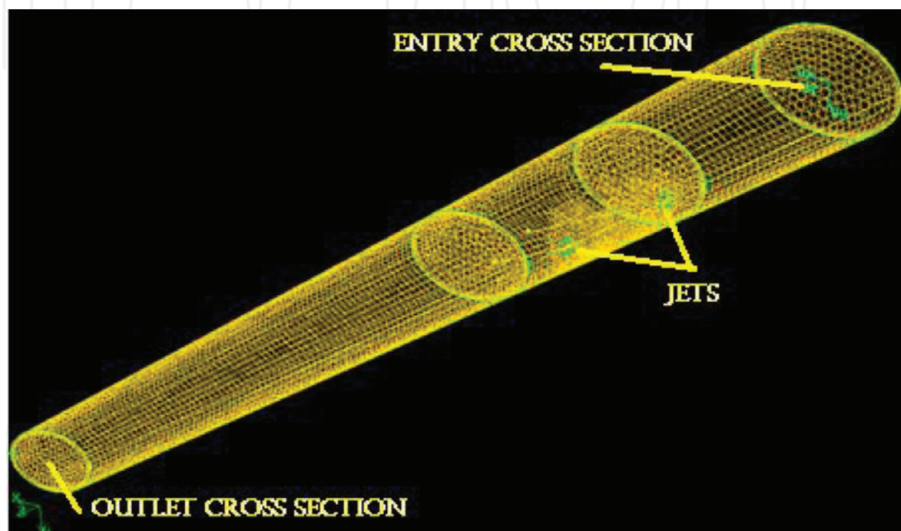
Figure 2.
Networked laryngoscope and 3D geometry.

The properties and quality of the resulting network are:

- 64.591 nodes, 104.056 volume elements.

- The aspect ratio was limited to a value of <5, except in the outer segments where a ratio of 10 was deemed acceptable (The aspect ratio is only greater than 3.6 in the outer segments.).

- The average skewness factor was limited to 0.33, and the maximum to 0.95 (0.17 and 0.94, respectively).

- The maximal squish index value was 0.99 (0.84).

1.1.3.1 Fluent

Fluent is a software solution utilizing the finite volume method to solve the problem at hand. Before the iterative solution process can be undertaken, certain settings with significant relevance need to be defined.

1.1.3.2 Settings

1.1.3.2.1 Solver

The pressure-based solver was selected.

1.1.3.2.2 Turbulence model

Because of the relatively high Reynolds values (44,000 and 28,000) of the laryngoscope entrance and exit zones, the airflow in the laryngoscope is turbulent. For numerical calculation the realizable k-E value was chosen, because the standard κ-ε model was not suited because of its weakness in calculation of sudden acceleration. Finally, the realizable κ-ε model was chosen

1.1.3.2.3 Species

Air and pure oxygen were defined as present substance in the presented model to determine the specific oxygen density at the exit diameter. The model allowed for the normal oxygen concentration of pure air (21%), because the Fluent software does not incorporate this correction factor automatically.

1.1.3.2.4 Boundary conditions

- Entrance diameter

Pressure inlet with surrounding pressure.
The utilized value is an approximation, due to the fact that the pressure upon entry is not constant, but depends on the pressure of both end stream nozzles. The higher the entrance velocity of the applied gas is, the higher the negative pressure of the entrance diameter becomes.

- Exit diameter

Pressure outlet with an assumed pulmonary pressure of 30/15 mbar

- Jets (nozzles)

Pressure inlet with 0.8 bar pressure at the low-frequency nozzle and 1.3 bar at the high-frequency aperture

- Wall

1.1.3.2.5 Solution controls

The settings of iteration, under-relaxation factors, and residuals were adapted to the stage of computation.

1.1.3.2.6 Steady flow

The pressures at both jets were assumed to be constant. The following conditions (**Table 1**) were analyzed.

1.1.3.2.7 Unsteady flow

The instationary current at the low-frequency nozzle is not constant, but varies between 0 and 1.3 bar, alternating every 2.5 sec. To accommodate this fact, a user-defined function (UDF) was programmed and added to the simulation. The pressure at the high-frequency nozzle was assumed to be constant.

To ensure accurate results for each time interval, each time interval should be short enough. Utilizing the Courant–Friedrichs–Lewy (CFL) value, every time step can be predicted sufficiently. The implied solver should be approximately 10.

$$\Delta t \;\; < \;\; CFLmin * \frac{\Delta x}{U}$$

Δx, element length; U, velocity.

Because the net is smallest and the velocity is highest as the nozzle exits, the time interval was estimated according to this data. This computes to Δt of 5e–6 s (Δx = 0.17 mm, U = 350 m/s), which in turn implies 20.000 intervals per second.

2.1 Results

Cases with stationary pressure with different pressure conditions and the effect of a stenosis were simulated. Simultaneous high- and low-frequency jet ventilation (Case A) is applied at an intrapulmonary pressure of 30 mbar. In this case, maximal velocities of 295 m/s could be measured at the low-frequency nozzle. The velocity

|	Pressure (low-frequency jet) [bar]	Pressure (high-frequency jet) [bar]
Case A	1.3	0.8
Case B	0	0.8
Case C	1.3	0

Table 1.
The pressure at both jets was assumed to be constant. The following conditions were analyzed. Case A was defined as the gas current during inspiration and expiration.

drops rapidly to a value of 43.2 m/s at the laryngoscope exit (**Figure 3**). The vector field (**Figure 4**) of the measured velocities of the high and low frequencies of gas current depicts the gas flow toward the lungs, and the simultaneous exit flows out of the lung contralaterally, allowing for an additional recirculation component on the opposite side of the nozzles. A negative pressure (**Figure 5**) is created due to the free jet characteristic of gas flow directly after having left the nozzle. These results in surround room air are sucked from the open end to the atmosphere.

2.2 Change in pulmonary pressure

Further simulation of the flow characteristics inside the jet laryngoscope, assuming a lower pressure in the lung (15 mbar). At first glance it is obvious the velocities along the z-axis rise (**Table 2**) when the opposite force in the lung is lower. The combined application of high- and low-frequency jet ventilation at
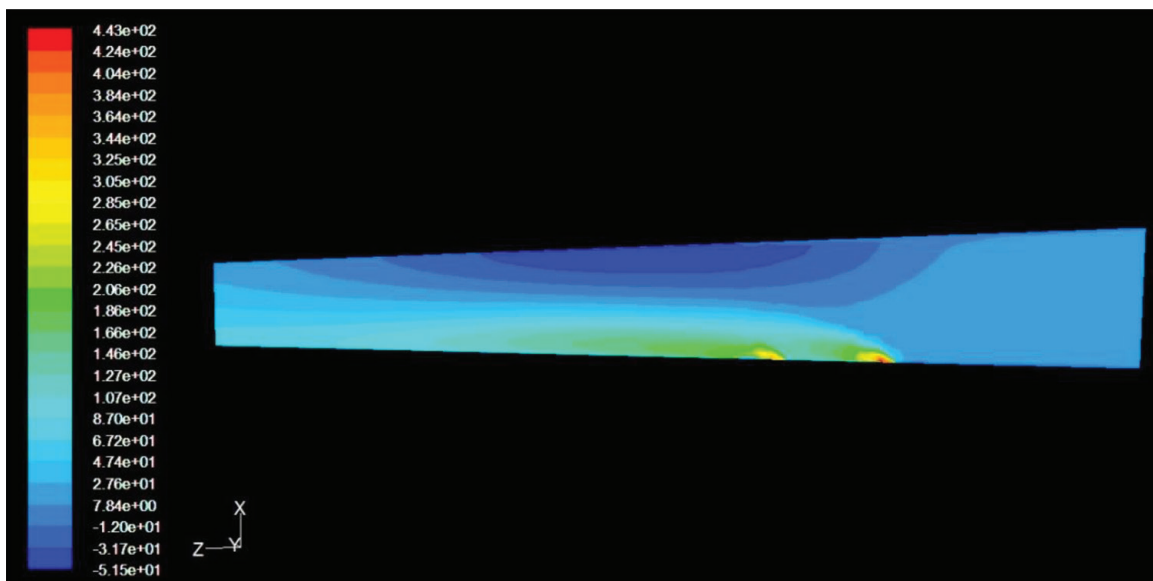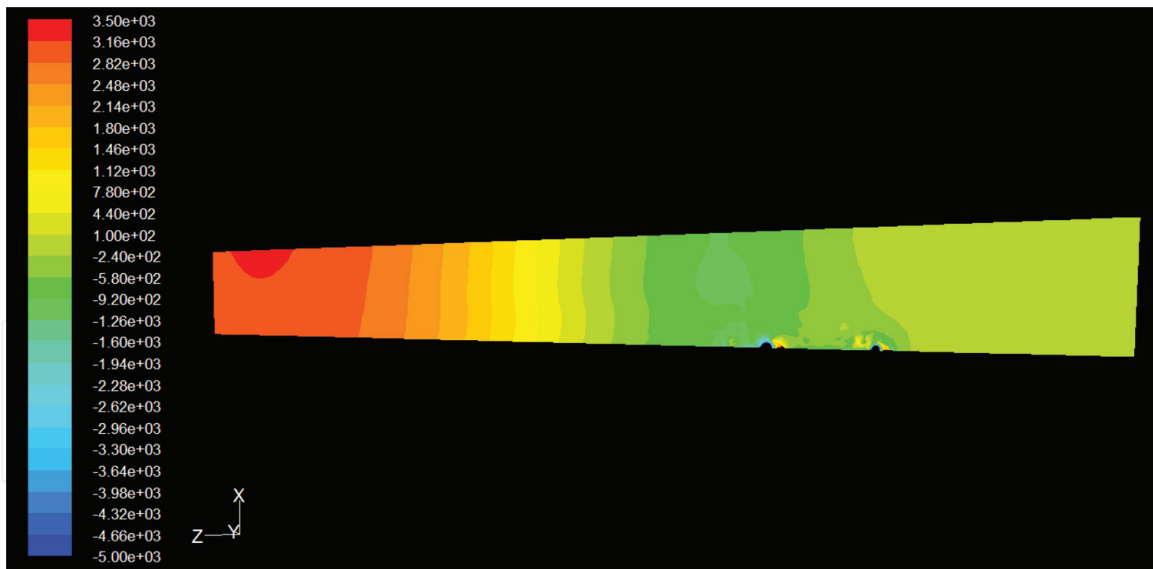

Figure 3.
z-component of velocity distribution (m/s). The influx of the gas takes place starting from the nozzle to the left. On the opposite side is the outflow of the gas.
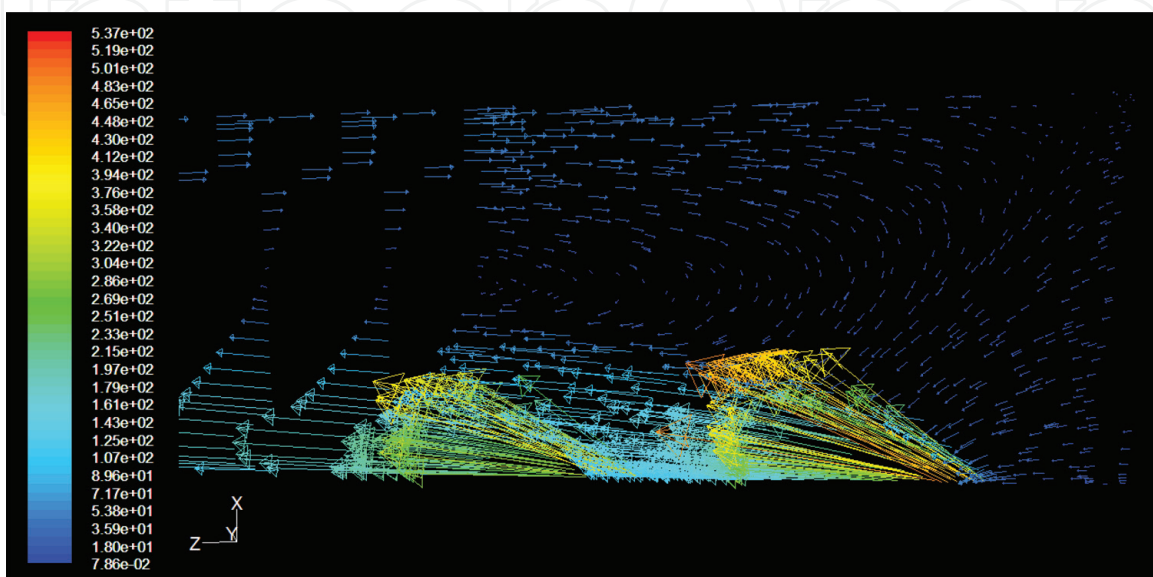
Figure 4.
Vector field of the velocity in the region of the two nozzle (m/s).

Figure 5.
Pressure distribution (the areas around the nozzles have been excluded due to the strong negative or high positive pressure of the color scale, to ensure that the pressure differences in the remaining region are more visible, pressure in Pa).

unchanged high "driving pressure" as in Case A shows that, with low pulmonary pressure (15 mbar), the velocities in the entrance and exit zones are markedly higher. Case C of single low-frequency jet ventilation exhibits a higher velocity as the single high-frequency jet (Case B) ventilation. However, the increased gas velocity results in a raised entrainment of air, reducing the oxygen concentration in the exit zone. **Table 3** shows that the mass transport is directly proportional to the velocities. **Figure 6** shows (Case A) the development of the gas flow with a lower intrapulmonary pressure. But here, too, there is a bidirectional gas flow.
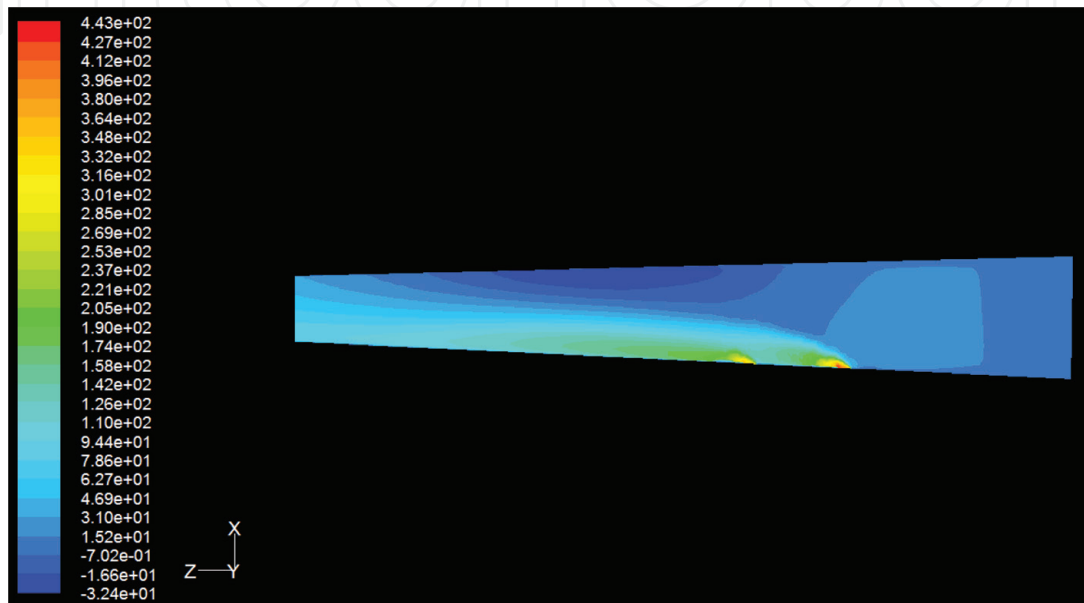
3. Stenosis

This simulation attempted to imitate laryngeal pathology with stenosis by reducing the cross section at the tip of the laryngoscope. In this study, a short yet circular stenosis was examined (**Figure 7**) similar to a clinical situation. The half-axes of the cross section were reduced from 7 to 4.5 mm and from 4 to 2.5 mm, which meant a reduction of 60% in diameter. For further simulation the system was extended after the stenosis by a piece of pipe. The remaining conditions are identical to Case A (combined high- and low-frequency jet ventilation). The intrapulmonary pressure

	v Exit	v Exit	v Entrance	v Entrance	O$_2$ Exit	O$_2$ Exit
	[m/s]	[m/s]	[m/s]	[m/s]	[%]	[%]
	15 mbar	30 mbar	15 mbar	30 mbar	15 mbar	30 mbar
Case A	58.38	43.51	Dez.89		48	53
Case B	23.27	−27.09	Apr.85	−10.03	42	22
Case C	38.99	15.55	Aug.75	Jän.90	50	57

Table 2.
Comparison of two different lung pressures (15 vs. 30 mbar). Behavior of flow velocities (m/s) and the oxygen content (%) at the entrance and exit of the jet laryngoscope at three different ventilation modes (Cases A, B, and C).

	Mass transport in the exit	Mass transport in the exit
	[kg/s]	[kg/s]
	15 mbar	30 mbar
Case A	−0.006892061	−0.0050869673
Case B	−0.002731038	0.003058461
Case C	−0.004529244	−0.001836674

Table 3.
Mass transport at the outlet cross section.

Figure 6.
*Velocity distribution for case A at 15 mbar pressure lung (m/s).*

Figure 7.
*Clinical situation of a circular stenosis just below the vocal cord level.*

was set at 15 mm. The reduction of ventilation diameter has the following implications: Proximal to stenosis the pressure rises (45 mbar), resulting in a reduction in velocity (approx. 20 m/s) before increasing once again (**Figure 8**) in the region of the stenosis and immediately post-stenotically (70 m/s) until a stable velocity of

25 m/s is reached. Simultaneously, there is a bidirectional gas flow in the laryngo-
scope again.

(**Figure 9**) shows the pressure distribution at the stenosis. The pre-stenotic
pressure corresponds to a dynamic pressure. It is important to note that despite the
pre-stenotic pressure being relatively high, there is an obligatory drop in post-
stenotic pressure (**Figure 10**). This results in an increase of lateral backflow and in
consequence reduced entrainment. (**Figure 11**) shows the vector field of the veloc-
ity in the area of stenosis. Localized recirculation can be seen. There is a backflow
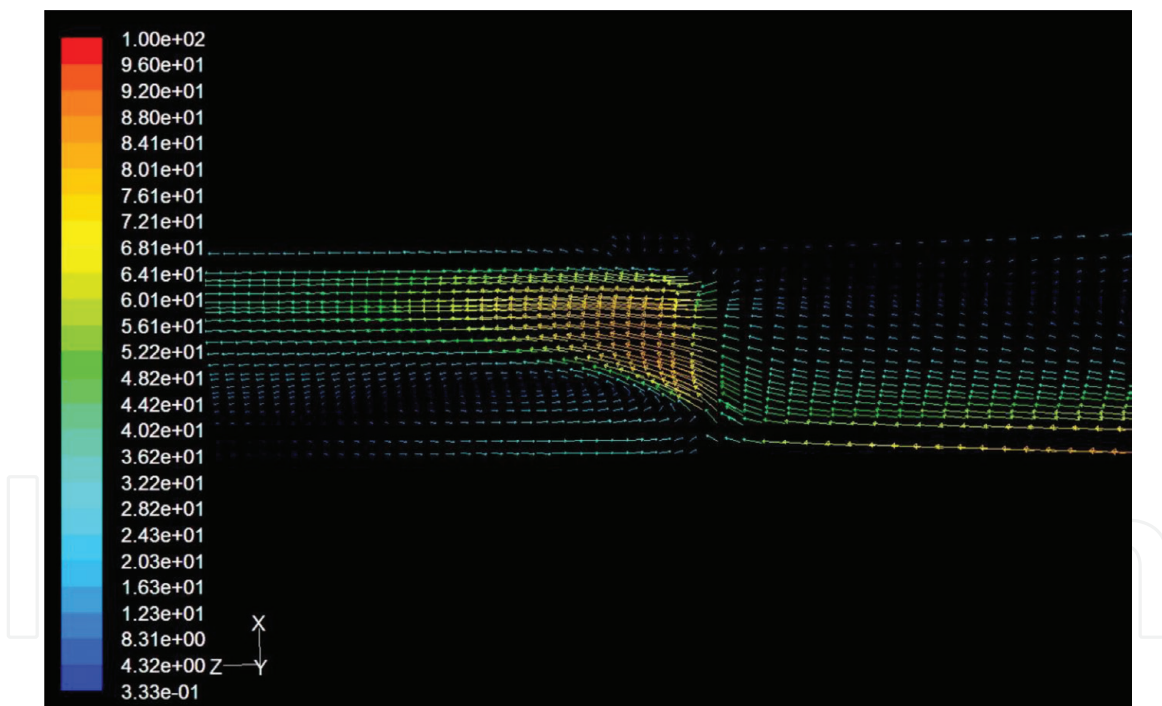both before and after the stenosis.
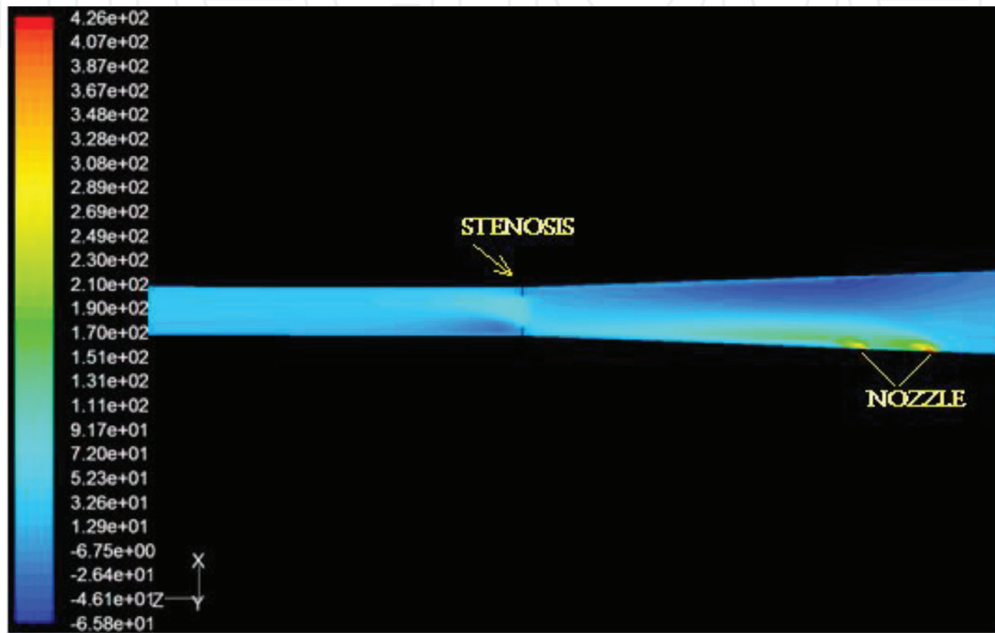
Figure 8.
*Velocity distribution in occurring stenosis at a pulmonary pressure from 15 mbar. At the side of the nozzle is a
high gas velocity. Simultaneously a gas discharge is on the opposite side (m/sec).*
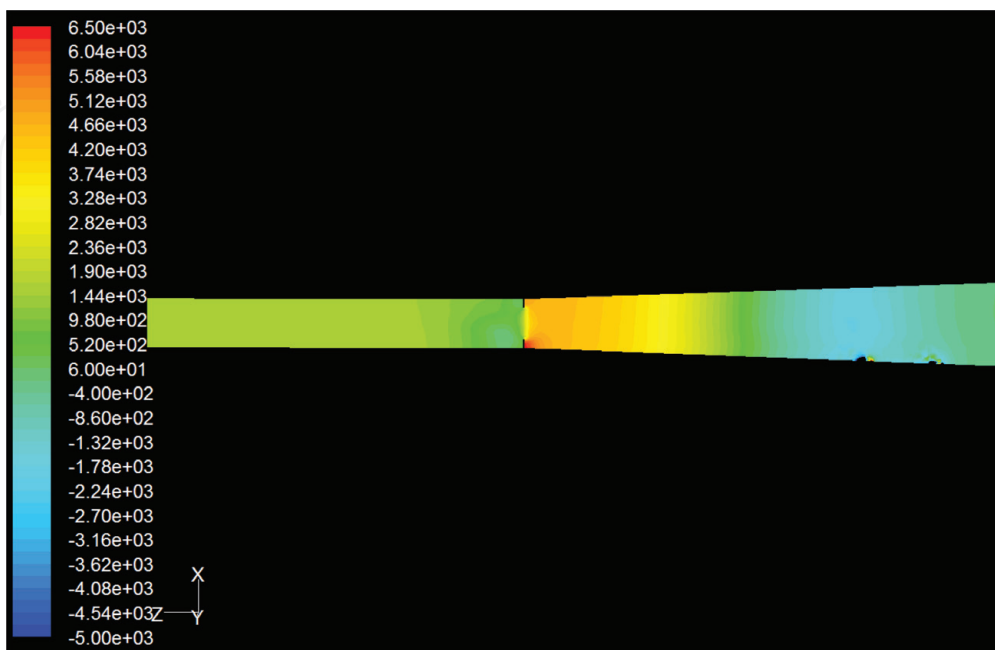
Figure 9.
*The pressure increases continuously in front of the stenosis, but he is lower in the area of the stenosis and after
the stenosis (Pa).*
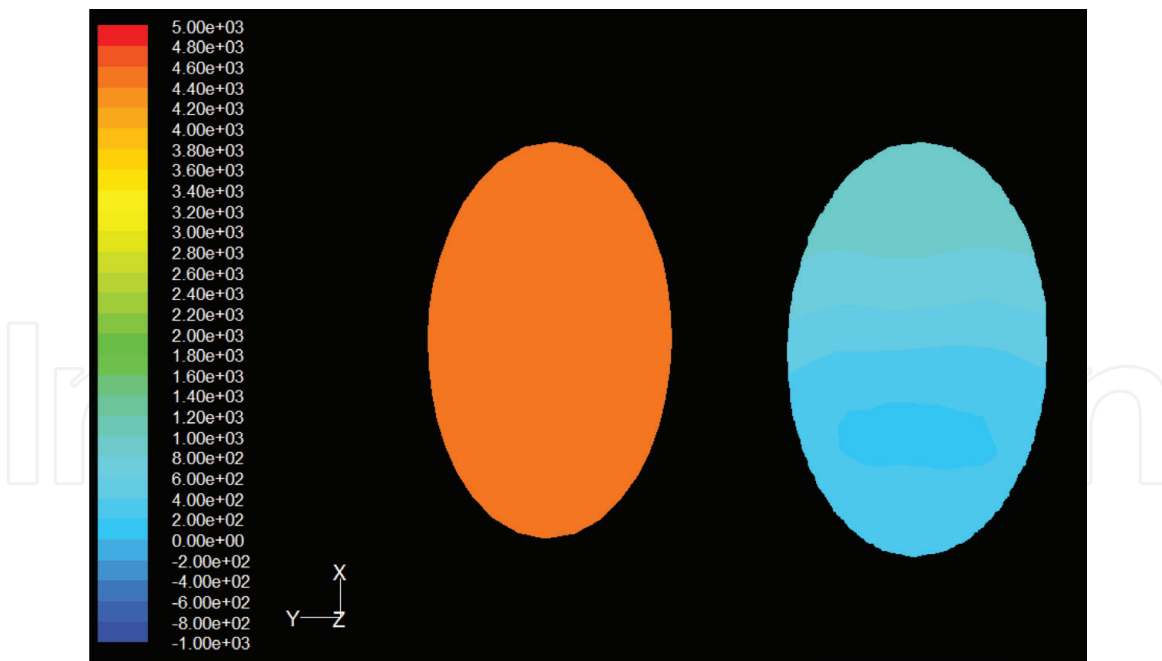
Figure 10.
Comparison of the pressure before (left) and after (right) the stenosis (note: For a better illustration of the pressure gradient over the cross section, the top and bottom values of the scale have changed).

Figure 11.
Backflows both before (top right) and after (bottom left) the stenosis.

4. Discussion

When reflecting on currents in tubes with round cross sections, a laminar airflow with parabolic velocity profile primarily springs to mind [13]. The current can present itself in a completely different matter and is illustrated by the airflow dynamics of the laryngoscope. Unique current patterns and pressure dynamics are created due to the technical specifications of the laryngoscope. Although the jet ventilation technique is a recognized and widely used method of jet ventilation technique [14, 15], no data on airflow and pressure dynamics have been published to date. As shown by

the data, both gas nozzles emit gas with the characteristics of a free jet [16, 17]. The free jet involving friction [18] then undergoes the typical expansion of the jet. While the nozzle produces a high entrance velocity, the velocity drops downstream due to energy loss of the projected fluid beam because of friction with the surrounding fluid. An entrainment [19] of air is induced at the edges of the laryngoscope due to the big difference in velocity between the free beam and the fluid in the laryngoscope. This, in turn, results in the reduction of oxygen by room air. Nevertheless, our results indicate that this entrainment includes a fraction of the projected gas, so that we could show an additional recirculation component of the projected gas when utilizing simultaneous high- and low-frequency jet ventilation. The lower the acceleration of airflow from the nozzles is, the smaller entrainment could be measured. These phenomena depend on the pressure of the jet gas, the gas velocity [20], and as Koller et al. [21] have already shown the localization of the jet nozzles.

As our results show, the gas flow can be described as asymmetrical and simultaneous bidirectional. The asymmetry is caused by the positioning of the jet nozzles. On the side of the nozzles, the jet gas flows in the direction of lungs with a high z-axis velocity. Even though the primary velocity of the emitted gas at the nozzle can be as high as 300 m/s, it reduces speed to 70 m/s at the tip of the endoscope. Because the velocity is only very high at the nozzle exit, it is acceptable to observe the common respiratory gases as incompressible fluids [22]. The term simultaneous bidirectional describes the synchronically process of gas transfer into the lung and from the lung by the continuous high-frequency jet ventilation. The low-frequency gas application takes place discontinuously.

4.1 Stenosis

The clinically relevant scenario of laryngeal or subglottic stenosis and obvious reduction of ventilation diameter (stenosis) is found at the tip of the endoscope. In contrast to previously publicized studies, which assume the nozzles of jet ventilation lie in close proximity to the tip of the endoscope [23], our supraglottic jet ventilation model uses the clinically accurate gas release point, located more proximally. Therefore, presuming that the previously published data is based on a gas release point of 1 cm proximal to the endoscope tip, this data is an incomparable data based on a proximal release point for supraglottic jet ventilation, which lies 6–8 cm proximally to the endoscope tip. Additionally, the pre-stenotic pressure plays an essential role in the gas passage through the stenotic pathology. It is not surprising that, as our results indicate, the pre-stenotic pressure drastically rises, while the velocity drops. The reduction in diameter is however also responsible for the increase in localized back draft and reduced entrainment. As we could show, there is also a pressure drop within the stenosis, which is also pronounced immediately after passage through the stenosis and continues for a finite distance post-stenotically. The fact that the pre-stenotic pressure is high and low in the post-stenotic area is not surprising from a fluid mechanical view. Our results show that in our case, the gas velocity drops pre-stenotically, just to rise again within the stenosis, only to drop again after the stenosis. The results demonstrate that the pressure during inspiration is higher in front of the stenosis than after the stenosis. Since stenosis represents an abrupt cross-sectional constriction, the Bernoulli equation may be included in fluid mechanical considerations only in enlargement by an operating element and pressure loss coefficient [24, 25]. Even though this physical law is widely known, many physicians and surgeons are unaware of its implication for laryngeal stenosis and often assume pressure to be higher post-stenotically [26].

5. Conclusion

Our results imply that if sole high-frequency gas dynamics can be compared to steady flow, then additional low-frequency gas flow should be seen as unsteady flow. It would be recommendable to investigate the transient case and add a user-defined function (UDF) to the calculation program to better understand and examine the gas flow within the laryngoscope. This notwithstanding, our data sheds new light on the flow patterns and dynamics of applied gas in the endoscope and contributes to a better understanding of jet ventilation as ventilation technique. This is especially true for the clinically highly relevant stenotic airway.

6. Respiratory devices

A new respiratory device (TwinStream, Carl Reiner, Vienna, Austria) has been developed for superimposed high-frequency jet ventilation (SHFJV) (**Figure 12**). Although the new technique is successfully used in clinical studies [27], there are few explanations about the structure and mechanism of the respirator. It is designed to allow both low-frequency and high-frequency jet ventilations simultaneously. An upper (plateau) and lower (positive end-expiratory pressure (PEEP) should be formed (**Figure 13**). The effectiveness of this combination causes an increased efficiency of gas exchange [28–30]. In addition, the ratio of inspiratory duration and expiratory duration (I/E ratio) can be determined. In contrast to previously used proportional valves, four matrix valves are used each. The gas of the central gas supply is mixed in the chambers—an algorithm recognizes the demand from the consumption (emission pressure, frequency, and I/E ratio) as well as the necessary oxygen mixture. Four matrix valves per medium (O2 and compressed air) tailed depending on the requirements and thus ensure the exact mixture. The chambers also allow intermediate storage and ensure that the gas output is constant and changes when the oxygen concentration changes.
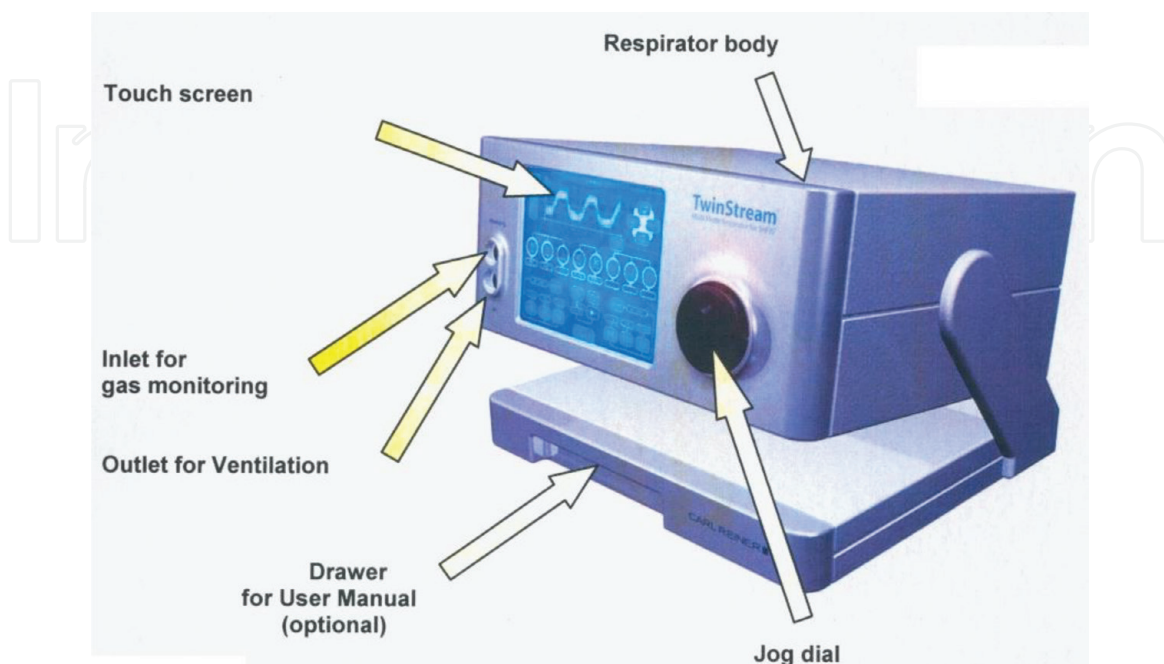
Figure 12.
Jet respirator (TwinStream).
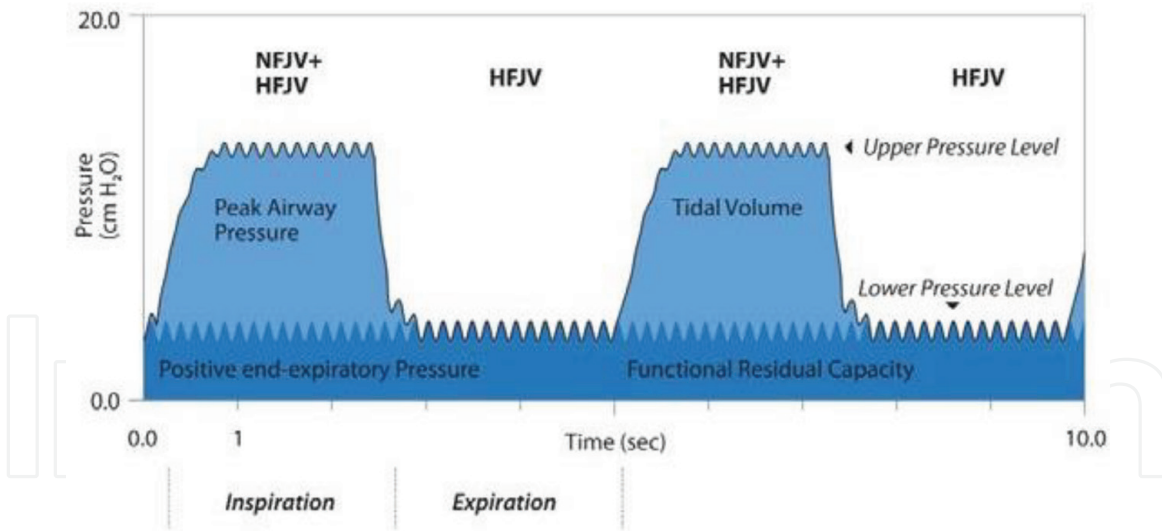
Figure 13.
Inspiration and expiration during SHFJV, NFJV – Normofrequent Jet Ventilation; HFJV – High Frequency Jet Ventilation.
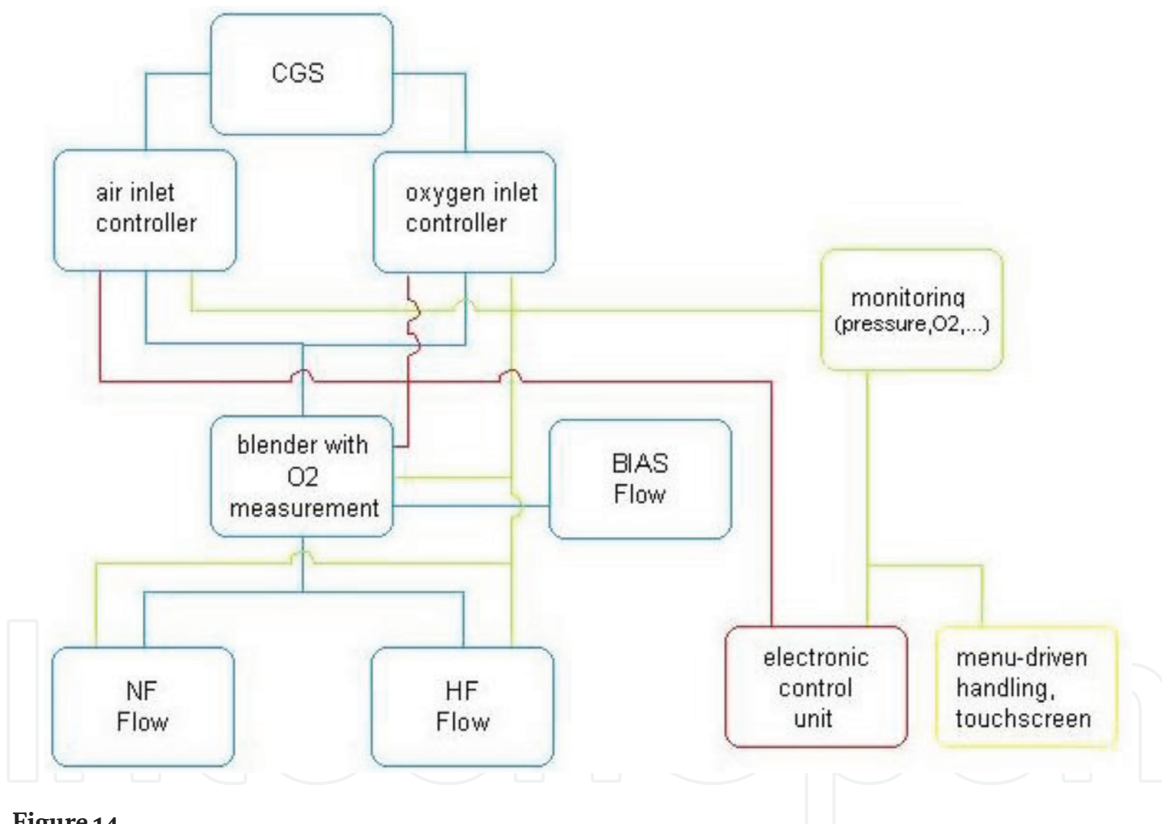
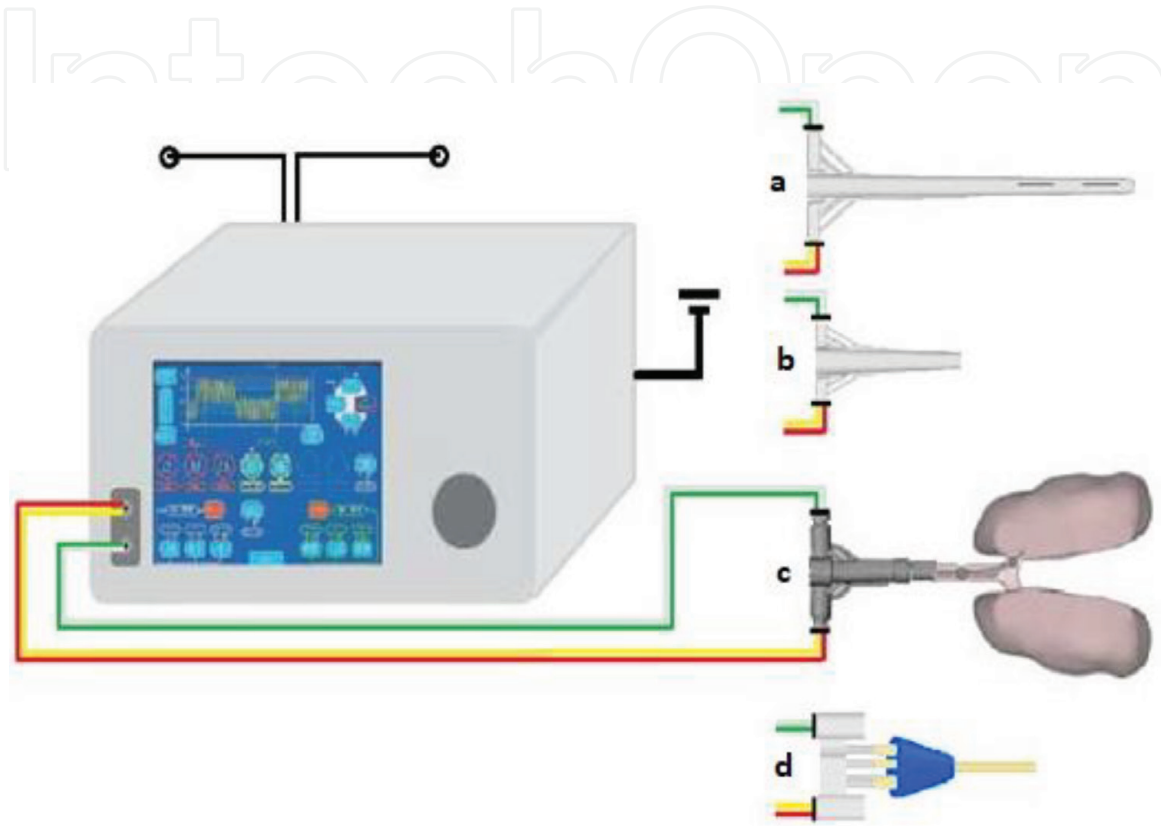**Figure 14.**
Respirator (TwinStream) pneumatic diagram.

The advantages of the matrix valves are the shortest switching times, no friction losses, and trouble-free generation of high frequencies. All parameters are controlled via a programmable logic controller (PLC). The frequencies and pressures that can be used in different ways have significantly extended the spectrum of the respiratory device. Since the gas coming from the nozzles is not humidified and warmed up, an additional gas flow is added to this gas (bias flow). This gas is heated and humidified by a humidifier (**Figure 14**).

In addition to its operational application, it can thus also be used in the intensive care with a jet modifier.

The superimposed high-frequency ventilation (SHFJV) respirator is flow-variable, time-controlled, and pressure-controlled ventilation. This form of jet

ventilation is closest to the conventional form of biphasic positive airway pressure ventilation. But it is a pulsatile ventilation. The low-frequency jet ventilation (NFJV) unit generates the upper pressure plateau during the inspiration phase (PIP—peak pressure). The high-frequency jet ventilation (HFJV) unit runs continuously and generates the lower-pressure plateau—positive end-expiratory pressure (PEEP).

The TwinStream jet ventilation system was developed for artificial ventilation of patients under anesthesia during diagnostic and surgical interventions in the

Figure 15.
TwinStream connection diagram for use with jet instrument rigid bronchoscope (a), jet instrument rigid laryngoscope (b), jet converter (c) that allows continuous ventilation through an endotracheal tube or a laryngeal mask, and jet catheter (d) which can also be used for ventilation.
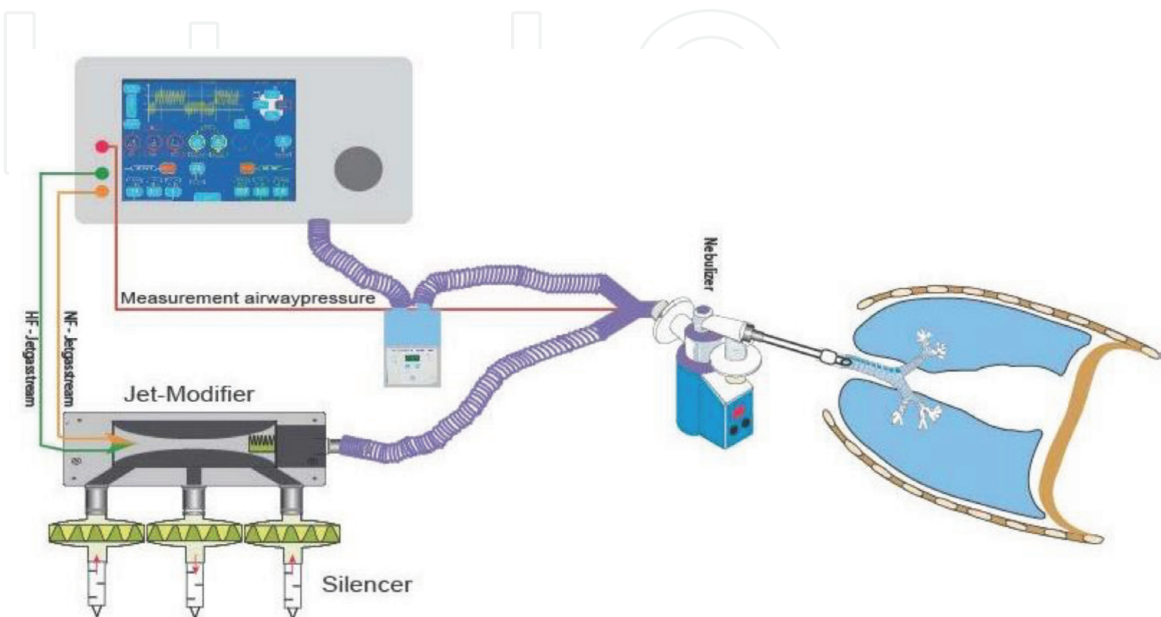
Figure 16.
Connection schematic for the use in the intensive care.

entire respiratory system. This ventilation system, with its special accessories and jet catheters, is appropriate for thoracic surgical use such as resection of the trachea (**Figure 15**). First, results show that this respirator is suitable for the treatment in patients with ARDS, lung fistulas, or multiple trauma at the intensive care unit. This advanced application requires a jet modifier (**Figure 16**). In this jet modifier, the superposition of the jet gas and its transport during the inspiration into the lungs as well as the gas outflow in the expiration phase take place.

In addition to jet ventilation, there is application of high-frequency oscillation in intensive care medicine [31, 32]. It is a recognized procedure. If small tidal volumes are emitted from a nozzle during jet ventilation, the tidal volumes are generated and transported at the high-frequency oscillation by vibrations of a membrane with a high frequency. Both techniques lead to an improvement in gas exchange. For a long time, it was believed that this improvement was due to increased diffusion mechanisms. Improved radiological techniques, however, show that they are due to a recruitment of alveoli.

Author details

Alexander Aloy[1], Simon Hell[1], Andreas Nowak[2*] and Matthaeus Grasl[3]

1 University of Technology Vienna, Institute of Fluid Mechanics and Heat Transfer, Vienna, Austria

2 Department of Anesthesiology and Intensive Care Medicine, Emergency and Pain Medicine, Hospital Dresden, Friedrichstadt, Germany

3 Department of Ear, Nose and Throat Diseases, Medical University of Vienna, Vienna Austria

*Address all correspondence to: alexander@aloy.at

IntechOpen

References

[1] Andersson B, Andersson R. Computational Fluid Dynamics for Engineers. Göteborg, Sweden: Cambridge University Press; 2011

[2] Yin Y, Ci J, Hoffmann EA, Tawhai MH, Lin C-L. Simulation of pulmonary air flow with a subject-specific boundary condition. Journal of Biomechanical Engineering. 2010;**43**:2159-2163

[3] Walters DK, Luke WH. Computational fluid dynamics simulations of particle deposition in large-scale, multigenerational lung models. Journal of Biomechanical Engineering. 2011;**133**(1). 8 pages

[4] Calkins JM, Waterson CK, Hameroff SR, Kanel J. Jet pulse characteristic for high-frequency jet ventilation in dogs. Anesthesia and Analgesia. 1982;**61**:293-300

[5] Orloff LA, Parhizkar N, Ortiz E. The Hunsaker Mon-jet ventilation tube for microlaryngeal surgery: Optimal laryngeal exposure. Ear, Nose, & Throat Journal. 2002;**81**:390-394

[6] Bourgain JL, Desruennes E, Fischler M, Ravussin P. Transtracheal high frequency jet ventilation for endoscopic airway surgery: A multicenter study. British Journal of Anaesthesia. 2001;**87**:870-875

[7] Barakate M, Maver E, Wotherspoon G, Havas T. Anaesthesia for microlaryngeal and laser laryngeal surgery: Impact of subglottic jet ventilation. The Journal of Laryngology and Otology. 2010;**124**:641-645

[8] Aloy A, Schachner M, Cancura W. Tubeless translaryngeal superimposed jet ventilation. European Archives of Oto-Rhino-Laryngology. 1991;**248**:475-478

[9] Sigloch H. Technische Fluidmechanik. Springer Dordrecht Heidelberg London NewYork: Springer Verlag; 2011

[10] Aloy A, Kimla T, Schrag E, Donner A, Grasl M. Tubuslose superponierte Hochfrequenz-Jet-Ventilation (SHFJV) bei hochgradigen laryngealen Stenosen. Laryngo-Rhino-Otol. 1994;**73**:405-411

[11] Depirerraz B, Ravussin P, Brossad E, Monnier P. Percutaneous transtracheal jet ventilation for paediatric endoscopic laser treatment of laryngeal and subglottic lesions. Canadian Journal of Anaesthesia. 1995;**42**:554-556

[12] Rezaie-Majd A, Bigenzahn W, Denk D-M, Burian M, Kornfehl J, Grasl MC, et al. Superimposed high-frequency jet ventilation (SHFJV) for endoscopic laryngotracheal surgery in more than 1500 patients. British Journal of Anaesthesia. 2006;**96**:650-659

[13] Surek D, Stempin S. Angewandte Strömungsmechanik für Praxis und Studium. Wiesbaden Germany: Teubner Verlag/GWV Fachverlage GmbH; 2007

[14] Aloy A, Schachner M, Cancura W. Tubuslose translaryngeale superponierte jet-ventilation. Der Anaesthesist. 1990;**39**:493-498

[15] Friedrich G, Mausser G, Gugatschka M. Die Jet-Ventilation in der operativen Laryngologie. HNO. 2008;**12**:1197-1206

[16] Schobeiri MT. Fluid Mechanics for Engineers: A Graduate Textbook. Berlin Heidelberg: Springer Verlag; 2010

[17] Durst F. Grundlagen der Strömungsmechanik: Eine Einführung in die Theorie der Strömungen von Fluiden. Berlin Heidelberg New York: Springer Verlag; 2006

[18] Schade H, Kunz E. *Strömungslehre*. Berlin: de Gruyter Verlag; 2007

[19] Pijush K, Ira MC. *Fluid Mechanics*. London Wall: Academic Press sn imprint of Elsevier; 2010

[20] Falcone AM, Cataldo JC. Entrainment velocity in an axisymmetric turbulent jet. Journal of Fluids Engineering. 2003;**125**(4):620-627

[21] Koller-Milosevic D, Schneider W. Free and confined jets at low Reynolds numbers. Fluid Dynamic Research. 1993;**12**(6):307-327

[22] Siekmann HE. Strömungslehre: Grundlagen. Berlin Heidelberg: Springer Verlag; 2000

[23] Ng A, Russell WC, Harvey N, Thompson JP. Comparing methods of high frequency jet ventilation in a model of Laryngotracheal stenosis. Anest Analg. 2002;**95**:764-769

[24] Kuhlmann HC. Strömungsmechanik. ein Imprint von Pearson Education München/Germany. Boston. San Francisco. Harlow, England: Paerson Studium; 2007

[25] Böswirth L, Bschorer S. Technische Strömungslehre: Lehr- und Übungsbuch. Springer Fachmedien Wiesbaden GmbH Germany: Vieweg u. Teubner; 2012

[26] Buczkowski PW, Fombon FN, Lin ES, Russsel WC, Thompson JP. Air entrainment during high-frequency jet ventilation in a model of upper tracheal stenosis. British Journal of Anesthesia. 2007;**99**:891-897

[27] Hohenforst-Schmidt W, Zarogoulidis P, Huang H, Man YG, Laskou S, Koulouris C, et al. A new and safe mode of ventilation for interventional pulmonary medicine: The ease of nasal superimposed high frequency jet ventilation. Journal of Cancer. 2018;**9**(5):816-833

[28] R S, LoMauro A, Gandolfi S, Priori R, Aliverti A, Frykholm P, et al. Influence of tracheal obstruction on the efficacy of superimposed high-frequency jet ventilation and single-frequency jet ventilation. Anesthesiology. 2015;**123**(4):799-909

[29] Jiang Y, Kacmarek RM. Efficacy of superimposed high-frequency jet ventilation applied to variable degrees of tracheal stenosis: One step forward to optimized patient care. Anesthesiology. 2015;**123**:747-749

[30] Putz L, Mayne A, Dincq. Jet ventilation during rigid bronchoscopy in adults: A focused review. Bio Med Research InternationaI. 2016. Article ID 4234861, 6 pages

[31] Xu-Xiong G, Zhao-Ni W, Ya-Ting L, Li P, Li-Fen Y, Yan H, Yue-Yu S, Liang-Ming C, Zhuang-Gui C. High-frequency oscillatory ventilation is an effective treatment for severe pediatric acute respiratory distress syndrome with refractory hypoxemia. Therapeutics and Clinical Risk Management. 2016;**12**:1563-1571

[32] Chang HK. Mechanism of gas transport during ventilation by high-frequency oscillation. Journal of Applied Physiology: Respiratory, Environmental and Exercise Physiology. Mar 1984;**56**(3):653-663